CONCEPTS FOR A THEORETICAL AND EXPERIMENTAL STUDY OF LIFTING ROTOR RANDOM LOADS AND VIBRATIONS

(Effects of Torsional Blade Flexibility on Single Blade Random Gust Response Statistics)

Phase V-A Report under Contract NAS2-4151

by

Kurt H. Hohenemser

and

Gopal H. Gaonkar

Department of Mechanical and Aerospace Engineering

Washington University
School of Engineering and Applied Science
St. Louis, Missouri

June, 1971

CONCEPTS FOR A THEORETICAL AND EXPERIMENTAL STUDY OF LIFTING ROTOR RANDOM LOADS AND VIBRATIONS

(Effects of Torsional Blade Flexibility on Single Blade Random Gust Response Statistics)

Phase V-A Report under Contract NAS2-4151

Prepared for the Ames Directorate, AMRDL,
at Ames Research Center, Moffett Field, California

by Kurt H. Hohenemser

Kurt H. Hohenemser

and Gopal H. Gaonkar

Gopal H. Gaonkar

Washington University
School of Engineering and Applied Science
St. Louis, Missouri

June, 1971

Scope of Contract NAS2-4151

Work under Contract NAS2-4151 started on February 1, 1967. Phase I Report of September 1967 develops analytical concepts for a random loads and vibrations analysis of lifting rotors. Phase II Report of August 1968 presents a perturbation solution method for random blade flapping. Phase III Report of June 1969 develops a more general method to include high rotor advance ratios and makes use of a specific atmospheric turbulence model. Phase IV Report of June 1970 extends the method to the computation of threshold crossing statistics for random blade flapping and introduces non-uniformity of the vertical turbulence velocity in the longitudinal direction. During FY 1971 the work was extended in three directions, resulting in 3 separate Phase V reports. Phase V-A Report covers the inclusion of blade torsional flexibility in the blade random gust response statistics. Phase V-B Report covers the analysis of lifting rotor gust alleviation methods and rotor dynamic stability. Phase V-C Report describes the efforts to develop experimental methods of substantiating the random loads and vibration analysis. The work summarized in Phase V-A Report was performed under Modification 5 to subject contract. The work summarized in Phase V-B and Phase V-C Reports was performed under Modification 6 to subject contract. A proposal has been submitted

for an extension of Contract NAS2-4151 through FY 1972 and FY 1973. The scope of the proposed extension is to remove some of the limitations of the present analytical model and at the same time simplify the method of analysis, and to conduct model tests to support the analysis.

CONCEPTS FOR A THEORETICAL AND EXPERIMENTAL STUDY OF LIFTING ROTOR RANDOM LOADS AND VIBRATIONS

Phase V-A

(Effects of Torsional Blade Flexibility on Single Blade Random Gust Response Statistics)

by

Kurt H. Hohenemser
and
Gopal H. Gaonkar

Washington University
St. Louis, Missouri

Abstract

The previously developed method of determining the flapping gust response statistics of a rigid blade flexibly hinged at the rotor center has been extended to include torsional blade flexibility. Quasi-steady aerodynamics have been assumed and a torsion mode where the amplitude is proportional to the distance from the rotor center. Under the assumptions made aerodynamic torsional moment inputs are limited to the region of reverse flow where the aerodynamic center and the section center of gravity are separated by half the blade chord. Thus negligible effects of blade torsional flexibility are obtained for rotor conditions with negligible reverse flow effects. Numerical examples refer to conditions with 1.6 rotor advance ratio. It was found that the random flapping

response is only moderately affected by the torsional flexibility, however large random torsional loads and deflections occur even if flapping is completely suppressed. The coupling of the actual flapping motion into the blade torsional motion produces a substantial increase in the random torsional loads or deflections.

CONCEPTS FOR A THEORETICAL AND EXPERIMENTAL STUDY OF LIFTING ROTOR RANDOM LOADS AND VIBRATIONS

Phase V-B

(Effects of Torsional Blade Flexibility on Single Blade Random Gust Response Statistics)

Table of Contents

List of Figures

Notation

V	flight velocity
R	rotor radius
Ω	angular rotor speed
t, t_1, t_2	time variables
ω, ω_1, ω_2	circular frequencies
L	scale of longitudinal turbulence
$s_{\lambda\lambda}(\omega)$, $s_{x_j x_j}(\omega)$	two-sided scalar power spectral densities for random functions $\lambda(t)$, $x_j(t)$, etc.
$s_{x_j x_k}(\omega)$	two-sided scalar cross-spectral density between random functions $x_j(t)$ and $x_k(t)$
$\mu = V/\Omega R$	rotor advance ratio
B	tip-loss factor
$a = 2\mu/(L/R)$	non-dimensional turbulence parameter
W	vertical turbulence velocity
$\lambda = W/\Omega R$	non-dimensional vertical turbulence velocity
β	blade flapping angle
δ	torsional deflection of blade tip
$P^2 = 1 + \omega_\beta^2/\Omega^2$	elastic flapping restraint parameter
$C(t), K(t), m_{\theta_1}(t), m_\lambda(t)$ $C_\delta(t), K_\delta(t), \ell_{r\beta}(t), \ell_{r\beta}(t)$ $\ell_{r\lambda}(t)$	periodic aerodynamic coefficients
γ	blade Lock inertia number
$f\Omega$	blade torsional frequency

I_l	flapping mass moment of inertia
I_f	feathering mass moment of inertia
c	blade chord
F, Q	non-dimensional quantities characterizing respectively the aerodynamic damping of the blade torsional deflections and the excitation of blade torsion by the lift of the reverse flow region, see Eq. (3-6)
$\dot{\beta}$, $\dot{\delta}$, $\dot{X}$	rate of change of β, δ, X, etc.
$\ddot{\beta}$, $\ddot{\delta}$	rate of change of $\dot{\beta}$, $\dot{\delta}$, etc.
$X(t)$	state or output vector
$A(t)$	state matrix
$B(t)$	coupling matrix
$F(t)$	stationary or non-stationary input random vector
$X^T(t)$, $A^T(t)$	transpose of X(t), A(t), etc.
$\Phi(t,\tau)$	state transition matrix
$W(t,\tau)$	weighting function or impulse response matrix
I_n	n x n identity matrix
$Y(\omega,t)$	output vector for $\lambda = e^{i\omega t}u(t)$, zero initial conditions
$Y^*(\omega,t)$	complex conjugate of $Y(\omega,t)$
$y_{jl}(\omega,t)$	a typical element of $Y(\omega,t)$
$y_{jlc}(\omega,t)$	real part of $y_{jl}(\omega,t)$
$y_{jls}(\omega,t)$	imaginary part of $y_{jl}(\omega,t)$
$\delta(\ldots)$	Dirac delta function
$E[\ldots]$	expected value
$R_{XX}(t_1,t_2)$	correlation matrix of X(t)

$R_{FF}(t_1,t_2)$	correlation matrix of F(t)
$S_{FF}(\omega_1,\omega_2)$	two-sided spectral density matrix of non-stationary F(t)
$S_{FF}(\omega)$	two-sided spectral density matrix of stationary F(t)
$R_{XX}(t,t)$	variance matrix of X(t) with typical diagonal elements $R_{x_j x_j}(t)$ and $R_{x_j x_k}(t)$
$\sigma_{x_j}(t) = \sqrt{R_{x_j x_j}(t)}$	standard deviation of $x_j(t)$
$r_{x_j x_k}(t)$	cross correlation coefficient between components x_j and x_k, see Eq. (2-23)
$p_{x_j x_k}(x_j,x_k,t)$	time variable joint probability density function between components x_j and x_k.
ξ	threshold for response components
$E[N_{+x_j}(\xi,t)]$	time variable expected number of positive crossings per unit time of threshold ξ for response component x_j
$E[M_{+x_j}(\xi)]$	expected number per rotor revolution of positive crossings of level ξ

1. Introduction

While all preceding work under subject contract presented in Phase I to IV reports and published in References (1) to (3) was limited to the analysis of the response variance and response level crossing statistics of a rigid flapping blade, the present report deals with the extension of this analysis to multidegrees of freedom systems, in particular to the inclusion of the torsional blade flexibility which in the high advance ratio regime with large regions of reverse flow has a significant effect on blade vibrations.

The general response correlation theory is formulated via the frequency response method using the state variable approach which is convenient to treat multidimensional systems with feedback systems and with several input components. However the algorithm for the digital computer program makes use of the fact that the same random excitation occurs at all inputs. Although some of the general derivations have already been published in Reference (3), they are included herein for the sake of completeness.

The numerical results for the example include both in blade torsion and in blade flapping, the mean square response values and the expected values of the rate of up-crossings for nine response levels of the combined random flapping and random blade torsion model. In order to study the coupling effects between blade flapping and blade torsion on the blade

response characteristics, these numerical results are also compared with the corresponding results from a one degree of freedom model in which only flapping or only torsional deflections are permitted.

According to the finding in the phase IV report, the effects of longitudinally non-uniform turbulence over the rotor plane are neglected and consequently the inflow excitation at the rotor center is taken as the representative of the vertical turbulence velocity distribution over the entire rotor disk. However, the assumption that the self-induced turbulence in the rotor plane can be neglected as compared to the turbulence of the free atmosphere is retained, and for computational purposes the Taylor-von Kármán turbulence spectrum has been approximated by an exponential low-pass type spectral density function. Though somewhat inaccurate, the assumption of quasi-static aerodynamics has been retained also for the coupled flapping-torsion problem. The errors from not using unsteady aerodynamics are probably comparable to those from using a simplified analytical rotor model with blades rigid in flap-bending and in chordwise bending. The results cannot be expected to be quantitatively correct, but they should provide the proper trends and valuable insights into the mechanism of the random gust response.

2. Response Covariance Matrix and Threshold Crossing Statistics

As indicated in Phase IV Report the state variable approach for multidimensional systems provides a computationally convenient and mathematically compact representation of the system dynamics. Therefore, preparatory to the description of the blade response covariance matrix via the method of harmonic inputs, we first introduce a state vector X(t). The number of components, or the dimension of X(t) would depend upon the number of degrees of freedom and the type of feedback systems. However, we stipulate that the state vector is of dimension n x 1 and that it is also identical to the response vector. Now, the linearized equations of motion of a lifting rotor system with finitely many degrees of freedom can be expressed in the state vector form

$$\dot{X} = A(t)X + B(t)F, \quad X(0) = 0, \quad 0 < t \leq T \qquad 2\text{-}1$$

or in index notation

$$\dot{x}_j = a_{jk}(t)x_k + b_{j\ell}(t)f_\ell, \quad j,k = 1,2,\ldots n \text{ and } \ell = 1,2,\ldots m \text{ and } n > m.$$

A(t) is the state or essential matrix which depends on the system damping and spring parameters, while the coupling matrix B(t) with elements representing the input modulating functions relates the input vector F(t) with the rate of state vector $\dot{X}(t)$. Referring again to equation (2-1), we now define the state transition matrix by

$$\frac{d\Phi}{dt}(t,\theta) = A(t)\,\Phi(t,\theta) \qquad 2\text{-}2a$$

with the initial conditions

$$\Phi(\theta,\theta) = I_n \qquad 2\text{-}2b$$

where I_n is a n x n identity matrix.

A typical jth column of the state transition matrix, $[\phi_{ij}]$, i = 1,2,...n, is the solution of the homogeneous equation (2-1) with F(t) = 0 and for the initial condition at t = θ

$$\begin{Bmatrix} x_1 \\ x_2 \\ \vdots \\ \dot{x}_j \\ x_{j+1} \\ \vdots \\ x_n \end{Bmatrix} = \begin{Bmatrix} 0 \\ 0 \\ \vdots \\ 1 \\ 0 \\ \vdots \\ 0 \end{Bmatrix}$$

For zero initial state, the solution of equation (2-1) is given by the superposition integral

$$X(t) = \int_0^t \Phi(t,\theta)\,B(\theta)F(\theta)d\theta \qquad (2\text{-}3)$$

The state vector being identical to the output, the weighting function or the impulse response matrix can be expressed as

$$\begin{aligned} W(t,\theta) &= \Phi(t,\theta)\,B(\theta) \quad t > \theta \\ W(t,\theta) &= 0 \qquad\qquad\quad t \leqslant \theta \end{aligned} \qquad (2\text{-}4)$$

Therefore, according to equation (2-4) the state vector now reduces to

$$X(t) = \int_0^t W(t,\theta)\, F(\theta)d\theta \qquad 2\text{-}5$$

When the input vector has zero mean values, from the linearity of the system, the output vector will also have zero mean values. Therefore the input and output covariance matrices are equal to their respective correlation matrices defined by

$$R_{FF}(t_1,t_2) = E[F(t_1)\, F^T(t_2)] \qquad 2\text{-}6$$

and

$$R_{XX}(t_1,t_2) = E[X(t_1)\, X^T(t_2)] \qquad 2\text{-}7$$

Inserting equation (2-5) into (2-7) one obtains with equation (2-6) the response covariance matrix

$$R_{XX}(t_1,t_2) = \int_0^{t_1} W(t_1,\theta)d\theta_1 \int_0^{t_2} R_{FF}(\theta_1,\theta_2)W^T(t_2,\theta_2)d\theta_2 \qquad 2\text{-}8$$

The weighting function matrix is of dimension n x m while $R_{FF}(\theta_1,\theta_2)$ is the m x m covariance matrix of the input process. According to the generalized Wiener-Khinchine relation this input covariance matrix can be considered as the double Fourier transform of the spectral density matrix $S_{FF}(\omega_1,\omega_2)$. With $R_{FF}(\theta_1,\theta_2)$ expressed in terms of spectral density, Eq. (2-8) takes the form

For stationary input processes

$$S_{FF}(\omega_1,\omega_2) = I_m\delta(\omega_2-\omega_1) \tag{2-14}$$

therefore Eq. (2-13) simplifies to

$$R_{XX}(t_1,t_2) = \int_{-\infty}^{\infty} Y^*(\omega,t_1)\, S_{FF}(\omega)\, Y^T(\omega,t)d\omega \tag{2-15}$$

or in index notation

$$R_{x_jx_p}(t_1,t_2) = \int_{-\infty}^{\infty} \sum_{\ell=1}^{m}\sum_{k=1}^{m} y^*_{j\ell}(\omega,t)s_{f_\ell f_k}(\omega)y_{kp}(\omega,t_2)d\omega$$

$$j,p = 1,2,\ldots,n. \tag{2-16}$$

By setting $t_1=t_2=t$ in the above equation one gets the elements of the state variance matrix which in real arithmetic simplify to

$$R_{x_jx_j}(t,t) = \sum_{\ell=1}^{m} 2\int_0^{\infty} [y^2_{j\ell c}(\omega,t) + y^2_{j\ell s}(\omega,t)]\, s_{f_\ell f_\ell}(\omega)d\omega$$

$$+ \sum_{\substack{\ell=1\\ \ell\neq k}}^{m}\sum_{k=1}^{m} 2\int_0^{\infty} [y_{j\ell c}(\omega,t)\, y_{jkc}(\omega,t) + y_{j\ell s}(\omega,t)y_{jks}(\omega,t)]$$

$$s_{f_\ell f_k}(\omega)d \qquad j = 1,2,\ldots,n \tag{2-17}$$

and

$$R_{x_jx_p}(t,t) = \sum_{\ell=1}^{m} 2\int_0^{\infty} [y_{j\ell c}(\omega,t)y_{p\ell c}(\omega,t) + y_{j\ell s}(\omega,t)y_{p\ell s}(\omega,t)]$$

$$s_{f_\ell f_\ell}(\omega)d\omega + \sum_{\substack{\ell=1\\ \ell\neq k}}^{m}\sum_{k=1}^{m} 2\int_0^{\infty} [y_{j\ell c}(\omega,t)y_{pkc}(\omega,t) + y_{j\ell s}(\omega,t)$$

$$y_{pks}(\omega,t)]\, s_{f_\ell f_k}(\omega)d\omega \qquad j,p = 1,2,\ldots,n \tag{2-18}$$

$$R_{XX}(t_1,t_2) = \int_0^{t_1} W(t_1,\theta_1)d\theta_1 \int_0^{t_2} \left[\int_{-\infty}^{\infty}\int_{-\infty}^{\infty} S_{FF}(\omega_1,\omega_2)e^{-i(\omega_1\theta_1-\omega_2\theta_2)} d\omega_1 d\omega_2\right] W^T(t_2,\theta_2)d\theta_2 \tag{2-9}$$

where $i = \sqrt{-1}$.

When the order of integration in the above equation can be interchanged the scalar harmonic functions $e^{-i\omega_1\theta_1}$ and $e^{i\omega_2\theta_2}$ can be considered in combination with the respective weighting function matrices $W(t_1,\theta_1)$ and $W^T(t_2,\theta_2)$, and the state covariance matrix can be expressed as

$$R_{XX}(t_1,t_2) = \int_{-\infty}^{\infty}\int_{-\infty}^{\infty} \left[\int_0^{t_1} W(t_1,\theta_1)e^{-i\omega_1\theta_1}\, d\theta_1\right] S_{FF}(\omega_1,\omega_2) \left[\int_0^{t_2} W^T(t_2,\theta_2)e^{i\omega_2\theta_2}\, d\theta_2\right] d\omega_1 d\omega_2 \tag{2-10}$$

Observe that the superposition integral shown in brackets are system responses to harmonic excitations; that is, the frequency response matrix

$$Y(\omega,t) = \int_0^t W(t,\theta)e^{i\omega\theta}d\theta \tag{2-11}$$

satisfies the state equation

$$\dot{Y}(\omega,t) = A(t)\, Y(\omega,t) + B(t)e^{i\omega t} \tag{2-12}$$

Substitution of Eq. (2-11) into (2-10) yields

$$R_{XX}(t_1,t_2) = \int_{-\infty}^{\infty}\int_{-\infty}^{\infty} Y^*(\omega_1,t_1)\, S_{FF}(\omega_1,\omega_2)\, Y^T(\omega_2,t_2)d\omega_1 d\omega_2 \tag{2-13}$$

where

$$y_{j\ell}(\omega,t) = y_{j\ell c}(\omega,t) + iy_{j\ell s}(\omega,t), \quad i = \sqrt{-1}$$

From the linearity of the system, $y_{j\ell c}(\omega,t)$ and $y_{j\ell s}(\omega,t)$ are also the deterministic system responses when the corresponding random input components are replaced respectively by cos ωt and sin ωt. Computationally this means, Eq. (2-12) has to be integrated 2m times to generate the n x m frequency response matrix, $Y(\omega,t)$ in real arithmetic. As mentioned earlier, a case of special interest in our lifting rotor study is when $f_1=f_2=\ldots=f_m=\lambda$, such that the input spectral density matrix $S_{FF}(\omega)$ in Eq. (2-15) is replaced by the scalar spectral density function $s_{\lambda\lambda}(\omega)$. Observe that this is only a special case of Eq. (2-12) in which the coupling matrix B(t) and the frequency response matrix $Y(\omega,t)$ reduce to n x 1 column vectors. With $\ell=k=1$ in Eqs. (2-17) and (2-18) we have

$$R_{x_j x_j}(t,t) = 2\int_0^\infty [y_{jc}^2(\omega,t) + y_{js}^2(\omega,t)]\, s_{\lambda\lambda}(\omega)d\omega \qquad j = 1,2,\ldots,n \quad (2\text{-}19)$$

and

$$R_{x_j x_p}(t,t) = 2\int_0^\infty [y_{jc}(\omega,t)\, y_{pc}(\omega,t) + y_{js}(\omega,t)\, y_{ps}(\omega,t)]\, s_{\lambda\lambda}(\omega)d\omega \qquad j,p = 1,2,\ldots,n \quad (2\text{-}20)$$

where, for a preset discrete value of ω, deterministic response $y_{jc}(\omega,t)$ and $y_{js}(\omega,t)$ are generated by solving Eq. (2-12) only twice.

In reliability and cumulative damage studies it is of importance to know, in addition to the mean square response levels, the variation of random response oscillations with respect to several preset thresholds or response levels. Such threshold crossing statistics or the expected value of the rate of up-crossings of thresholds are required in the design of fatigue tests and to estimate fatigue allowables etc. Under certain conditions it is also possible to estimate the distribution of response peaks and the total expected damage within a given time interval; for details see Powell's formula on the distribution of high level peaks in reference (6) and Roberts' analysis (7) on cumulative damage due to non-stationary random loading.

Let x_j and x_k be two typical components of the response vector X(t) in equation (2-1) such that $\dot{x}_j = x_k$. Then, the expected value of the number of positive or up-crossings of response level ξ per unit time is given by the Rice Equation (8)

$$E[N_{+x_j}(\xi,t)] = \int_0^\infty x_j p_{x_j x_k}(\xi, x_k, t)\, dx_k \qquad (2\text{-}21)$$

When the input vector F(t) in Eq. (2-1) is jointly Gaussian, from the linearity of the system, the output vector is also jointly Gaussian and the joint probability density function $p_{x_j x_k}(x_j, x_k, t)$ between x_j and x_k is given by (reference 8)

$$p_{x_j x_k}(x_j,x_k,t) = \left(\frac{1}{2\pi}\,\sigma_{x_j}\sigma_{x_k}\right)\sqrt{1-r^2_{x_j x_k}}\;\exp\left[-\left\{\sigma^2_{x_j} x_k - 2\sigma_{x_j}\sigma_{x_k} r_{x_j x_k} x_j x_k + \sigma^2_{x_k} x_j^2\right]\middle| 2\sigma^2_{x_j}\sigma^2_{x_k}\sqrt{1-r^2_{x_j x_k}}\right\} \quad \ldots.(2\text{-}22)$$

Inserting equation (2-22) with $x_j = \xi$ into equation (2-21) and performing the integration over dx_k one obtains (Reference 8)

$$E[N_{+x_j}(\xi,t)] = \left[\frac{1}{2\pi}\sqrt{1-r^2_{x_j x_k}}\left(\frac{\sigma_{x_k}}{\sigma_{x_j}}\right)\exp\left\{-\left(\frac{\xi}{\sigma_{x_j}}\right)^2 \Big/ 2(1-r^2_{x_j x_k})\right\}\right] + \frac{1}{2\sqrt{2\pi}}\left(\frac{\sigma_{x_k}}{\sigma_{x_j}}\right)\left(\frac{\xi r_{x_j x_k}}{\sigma_{x_j}}\right)\left[\left\{\exp\left(-\left(\frac{\xi^2}{2\sigma^2_{x_j}}\right)\right)\right\}\left\{1 + \operatorname{erf}\left(\xi r_{x_j x_k}\middle|\sigma_{x_j}\sqrt{2(1-r^2_{x_j x_k})}\right)\right\}\right] \quad (2\text{-}23)$$

where

$$\sigma^2_{x_j} = E[x_j x_j]$$

$$\sigma^2_{x_k} = E[x_k x_k]$$

$$r_{x_j x_k} = \frac{E[x_j x_k]}{\sigma_{x_j}\sigma_{x_k}}$$

and

$$\operatorname{erf}(\theta) = \frac{2}{\sqrt{\pi}}\int_0^\theta e^{-t^2}\,dt.$$

3. Deterministic Response

The analytical model used for this study is described in the following. A centrally arranged flapping hinge with an elastic flapping restraint and linearized quasi-steady aerodynamics with reverse flow effects are stipulated. The dynamic equations of motion of such a flapping blade including the study of stability boundaries are given by Sissingh in Reference (4). In the present report we relax the assumption that the blade is rigid in torsion by considering the problem of combined random flapping and random blade torsion. Therefore, we briefly describe below the dynamic equations of the blade model, following the analysis of Sissingh and Kuczynski (5).

Under the stipulations stated earlier and further assuming a linear approximation for the normalized torsional mode shape the dynamic equations of blade flapping and blade torsion read (5)

$$\frac{2}{\gamma}\ddot{\beta} + C(t)\dot{\beta} + [\frac{2p^2}{\gamma} + K(t)]\beta - m_{\theta_1}(t)\delta = m_\lambda(t)\lambda \qquad (3\text{-}1)$$

$$\frac{1}{3\gamma}\ddot{\delta} + FC_\delta(t)\dot{\delta} + [\frac{f^2}{3\gamma} + QK_\delta(t)]\delta + Q\ell_{r\dot{\beta}}(t)\dot{\beta} + Q\ell_{r\beta}(t)\beta = -Q\ell_{r\lambda}(t)\lambda \qquad (3\text{-}2)$$

The time unit t is selected in such a way that the rotor angular velocity is one and the period of one rotor revolution is 2π. At an advance ratio greater than the tip-loss factor the time variable system parameters C(t), K(t) etc. in Eq. (3-1)

and (3-2) are non-analytic due to reverse flow. Therefore these system parameters are approximated by truncated Fourier series valid over the entire rotor disk. Assuming an advance ratio of 1.6 and a tip-loss factor of 0.97 we present in Figures 1a and 1b the system parameters $m_{\theta_1}(t)$, $C_\delta(t)$, $K_\delta(t)$, $\ell_{r\beta}(t)$, $\ell_{r\dot{\beta}}(t)$ and $\ell_{r\lambda}(t)$. For system parameters C(t), K(t) and $m_\lambda(t)$ which pertain to the pure flapping equation see Reference (2), pages 420 and 421. p in Eq. (3-1) represents the elastic flapping restraint parameter which is equal to one for zero flapping hinge offset and zero flapping restraint, while a hingeless rotor can be simualted with $p > 1$. For rotors with an elastic root restraint, p increases with decreasing rotor speed:

$$p^2 = 1 + (\omega_\beta/\Omega)^2 \tag{3-3}$$

The inflow ratio λ in Eq. (3-1) represents the vertical component of the turbulence with zero mean value and with the low-pass type exponential spectral density function. $m_\lambda(t)$ and $\ell_{r\lambda}(t)$ are called the input modulating functions.

For the sake of brevity we now introduce the notation

$$\frac{\gamma}{2}C(t) = D\beta_1(t),\ \frac{\gamma}{2}\left[\frac{2p^2}{\gamma} + K(t)\right] = S\beta_1(t)$$

$$\frac{\gamma}{2}\, m_{\theta_1}(t) = S\delta_1(t),\ \frac{\gamma}{2}\, m_\lambda(t) = A_\beta(t) \tag{3-4}$$

$$3\gamma\, FC_\delta(t) = D\delta_2(t),\ 3\gamma\left[\frac{f^2}{3\gamma} + QK_\delta(t)\right] = S\delta_2(t)$$

$$3\gamma\, \ell_{r\beta}(t) = S\beta_2(t),\ 3\gamma Q\ell_{r\dot{\beta}}(t) = D\beta_2(t) \text{ and } -3\gamma Q\ell_{r\lambda}(t) = A_\delta(t)$$

With the selected state vector

$$\beta = y_1,\ y_2 = \dot{\beta},\ y_3 = \delta \text{ and } y_4 = \dot{\delta} \tag{3-5}$$

the blade flapping and torsion equations (3-1) and (3-2) now take the form

$$\begin{Bmatrix} y_1 \\ y_2 \\ y_3 \\ y_4 \end{Bmatrix}^{\bullet} = \begin{bmatrix} 0 & 1 & 0 & 0 \\ -S\beta_1(t) & -D\beta_1(t) & S\delta_1(t) & 0 \\ 0 & 0 & 0 & 1 \\ -S\beta_2(t) & -D\beta_2(t) & -S\delta_2(t) & -D\delta_2(t) \end{bmatrix} \begin{Bmatrix} y_1 \\ y_2 \\ y_3 \\ y_4 \end{Bmatrix} + \begin{Bmatrix} 0 \\ A_\beta(t) \\ 0 \\ A_\delta(t) \end{Bmatrix} \lambda \tag{3-6}$$

As the state vector is identical to the response vector, $y_{jc}(\omega,t)$ and $y_{js}(\omega,t)$ in Eqs. (2-19) and (2-20) could be obtained by solving the matrix Eq. (3-6) with $\lambda = \cos \omega t$ and with $\lambda = \sin \omega t$ respectively.

In Figure 2, solid lines represent two typical response histories of $y_{1c}(0,t)$ and $y_{3c}(0,t)$ or according to Eq. (3-5) the flapping and torsional deflections to modulated step inputs. The dotted lines in the same figure refer to the uncoupled system obtained by setting $S\delta_1(t)$, $S\beta_2(t)$ and $D\beta_2(t)$ to zero in Eq. (3-6). The assumed set of system parameter constants which will be retained in subsequent numerical studies are given below

$\mu = 1.6$, $B = 0.97$, $\gamma = 4$, $p = 1.3$, $f = 8$, $F = 0.24$ and $Q = 15$.

Since $F = \dfrac{I_1}{I_f}\left(\dfrac{c}{R}\right)^2 \dfrac{1}{16}$ and $Q = \dfrac{c}{R}\ \dfrac{I_1}{I_f}\dfrac{1}{4}$,

if the lift slope for normal and reversed flow is assumed to be the same, the selected parameter values for F and Q correspond to a radius over chord ratio of (R/c) = 15.6 and to a ratio of flapping moment of inertia over feathering moment of inertia of $(I_l/I_f) = 940$. For these constants, according to the stability analysis of Sissingh and Kuczynski (5) the system is well within the stability region; see also Figure 8 of Reference (5). As expected $y_\beta(0,t)$ values of the uncoupled system agree with the corresponding flapping response histories shown in Figure 5 of Reference (2).

The computer solutions were obtained by a Runge-Kutta library subroutine with three timewise step-sizes: $\Delta t = 0.2$, 0.1 and 0.05. The numerical results with $\Delta t = 0.1$ and 0.05 were in good agreement, while the step-size of 0.2 was found to be unsatisfactory. Therefore this timewise step-size of 0.1 is maintained for all the numerical work presented in this phase V-A report. From Figure 2 it is evident that the coupling of torsional blade flexibility with blade flapping amplifies pure torsional step input amplitude by about 61%, while the coupled flapping response is affected only to a minor degree. This maximum amplification of torsional deflections occurs close to the central portion of the reversed flow region which for our blade model, during the second rotor revolution, lies within the azimuth range $3.2\pi \leqslant t \leqslant 3.8\pi$. The steady state is reached almost after the first rotor

revolution and the average flapping amplitude value of the coupled system agrees well with that given by Sissingh and Kuczynski (5).

4. Random Response

The computer results pertain to the combined random flapping and random torsion model for which the modulated step input response history is shown in Figure 2. The assumed spectral density function of the vertical inflow, which is the only type of input treated here, is given by

$$s_{\lambda\lambda}(\omega) = \frac{a}{\pi(a^2+\omega^2)} \qquad \text{for } \omega \leqslant 3$$

$$s_{\lambda\lambda}(\omega) = 0 \qquad \text{for } |\omega| \geqslant 3$$

For the assumed value of turbulence scale over rotor radius of (L/R) = 12 one obtains (Reference 2)

$$a = 2\mu/(L/R) = .266$$

The response statistical description includes root mean square values of the torsional and flapping deflections and the expected values of the rate of up-crossings for several response levels. Only the second rotor revolution is shown where the response variance matrix has become approximately periodic with period 2π. Further, in the comparison of response description between the coupled and uncoupled systems, full lines refer to the flapping blade with torsional

flexibility, while the dotted lines to the uncoupled system in which only flapping or torsional deflections are permitted. This latter case is obtained by setting the coupling parameters $S\delta_1$, $S\beta_2$ and $D\beta_2$ to zero in Eq. (3-1) and (3-2). The mean values of response up-crossings are obtained from Eq. (2-23) in which the response variance values of β, $\dot{\beta}$, δ and $\dot{\delta}$ are computed from Eq. (2-19) and the cross-covariance functions $R_{\beta\dot{\beta}}(t,t)$ and $R_{\delta\dot{\delta}}(t,t)$ from equation (2-20). A step-size of 0.1 was selected both with respect to time and frequency, and the required computer time on IBM 360/50 machine is about 12 minutes to cover 9 response levels.

In Figures 3 and 4, the root mean square values of the flapping and torsional deflections are given. It is instructive to note that the coupling between blade flapping and blade torsional flexibility influences $\sigma_\beta(t)$ values only to minor degree, where as its effect on $\sigma_\delta(t)$ is significant; the increase in the peak value of $\sigma_\delta(t)$ is of the order of 33%, when $t \approx 3.4\pi$. As expected this location of the peak value is close to the central portion of the reverse flow region which for our blade model lies within the azimuth range of 3.2π to 3.8π.

At this stage, it is worth comparing between $\sigma_\beta(t)$ and $|y_\beta(0,t)|$, and between $\sigma_\delta(t)$ and $|y_\delta(0,t)|$. As noted on page 423 of Reference 2, the absolute values of system response components to modulated step inputs shown in Figures 5a and 5b, could be respectively treated as the root mean

square response values for the limiting case of $L/R = \infty$, which is simple to interpret and economical to compute. From the study of Figures 3 and 5a, it is seen that $|y_\beta(0,t)|$ is a fairly satisfactory engineering approximation to $\sigma_\beta(t)$, the error with respect to the maximum value is roughly 16.5% even with the inclusion of torsional flexibility. Interestingly enough, the order of percentage error between $\sigma_\beta(t)$ and $|y_\beta(0,t)|$ is more or less the same both for the coupled and uncoupled systems, see also Figure 6 of Reference (2). However, from Figures 4 and 5b, what is significant is not so much the 28.5% error with respect to the peak values of $\sigma_\beta(t)$ and $|y_\delta(0,t)|$ of the coupled system, but it is the significant discrepancy in the pattern of variation. For the corresponding uncoupled system, see Figures 2 and 4, $\sigma_\beta(t)$ and $|y_\delta(0,t)|$ values agree well with respect to the maximum peak values, even though the pattern of variation differs significantly. Thus, from the view point of establishing certain design parameters of gust alleviating feedback systems etc., it appears that the limiting case of $L/R = \infty$ is satisfactory to approximate the flapping response variance values, at least for high altitude flight conditions where the turbulence scale length is much larger than the rotor radius. However, a similar approximation for torsional deflections could introduce large errors.

Figures 6 and 7 show the expected value of the rate of up-crossings for response levels zero and one. Figure 6a

in particular shows that the inclusion of the torsional flexibility has the effect of reducing sharp peaks in $E[_{+N\beta}(0,t)]$ most of which for the uncoupled system occur within a narrow range of the azimuth angle. In other words, for a given value of L/R the sample functions of random flapping of a blade with torsional flexibility would deviate more from the response histories to modulated step inputs than the response sample functions of a pure rigid blade flapping. Both Figures 6a and 6b indicate that for $\xi = 0$ and $\xi = 1$, the expected number of positive flapping crossings per rotor revolution or $E[M_{+\beta}(\xi)]$, is more or less the same for both coupled and uncoupled systems.

In Figures 7a nad 7b, as in Figure 6, the mean values of the rate of up-crossings of random torsional deflections are shown for threshold levels of zero and one. It is seen that the average value of the total number of zero crossings per revolution or $E[M_{+\delta}(0)]$, is higher for the uncoupled system. But, at $\xi = 1$, the coupled system will have a higher value of $E[M_{+\delta}(1)]$ than the uncoupled one. It is also interesting to note that for both the coupled and uncoupled systems $E[N_{+\delta}(0,t)]$ and $E[N_{+\delta}(1,t)]$ have sharp peaks at locations at which $y_{\delta}(0,t)$ crosses the response levels of zero and one with positive slope.

At this stage we revert back to certain observations on page 423 of Reference (2). It was stated that positive and negative turbulence velocities occur on the average with equal frequency so that during some rotor revolutions the

response for L/R = ∞ will look like a curve in Figure 2a; for an equal number of revolutions the response will be given by the mirror image of this curve. For finite values of L/R, zero crossings can occur at any time, with the most likely occurrence close to those for L/R = ∞. To gain further insight into the variation of response sample functions two response levels equidistant from the mean zero level are selected, the particular values of ξ in Figures 8a and 8b being ±1.75. Observe that for both coupled and uncoupled systems the peak value of $E[_{N_+\beta}(1.75,t)]$ occurs when $t \simeq 8.75$. Similarly for the uncoupled system the major peak value of $E_{+N_\beta}(-1.75,t)$ is in the neighborhood of t = 10.7. However, for the coupled system most of the up-crossings with respect to the response level of -1.75 occur when t varies from 10.6 to 11.6. It is instructive to study Figures 8a and 9b in conjunction with Figure 2a. It is evident that for both the coupled and uncoupled systems $y_\beta(0,t)$ values up-cross the response level of 1.75 when $t \simeq 8.75$. The mirror image of this response history also up-crosses ξ = -1.75 at $t \simeq 10.7$ for the uncoupled system, and for the coupled system response $y_\beta(0,t)$ with positive slope is almost at the level of -1.75 when t varies from 3.5π to 3.6π.

Figures 9a and 9b once again refer to the level crossing statistics, $-E[_{+N_\delta}(\pm 1.75,t)]$. The mirror image concept mentioned earlier is approximately true for torsional oscillations, even though one has now to consider up-crossings at close azimuth locations.

In Figure 10 the study of flapping response up-crossing statistics is further pursued by selecting higher response levels. A significant observation is the negligible difference between coupled and uncoupled systems in $E[N_{+\beta}(\xi,t)]$ values for $\xi \geq 2$. Observe also that $y_\beta(0,t)$ values of coupled and uncoupled systems are almost identical for response levels higher than 2, see Figure 2a. However, Figure 10 clearly indicates that random flapping response peaks, both for the coupled and uncoupled systems, reach much higher thresholds than what is shown by $y_\beta(0,t)$ in Figure 2a. Observe that in Figure 10 with t varying from 9 to 10, a few response peaks indicate the possibility of up-crossing a threshold level of 6, which is about 2.15 times higher than the maximum positive flapping amplitude of $y_\beta(0,t)$.

In order to relate the non-dimensional response levels used here to dimensional quantities it should be noted that according to Reference (2) a standard deviation of vertical gust velocity of 8 ft/s occurs at low altitude with about .1% probability. For 300 ft/s blade tip speed and 280 knots, giving $\mu = 1.6$, this results in $\sigma_\lambda = 1.5°$. The levels of β and δ indicated in the figures are then to be multiplied by 1.5 and interpreted as degrees. It is seen that a ζ-level of 6 corresponds to a blade tip torsional deflection of 9°, and very high random torsional deflections and loads will occur in turbulence even with a blade of high stiffness as indicated by the assumed torsional frequency f = 8 per rev.

In Figures 11 and 12, the threshold crossing statistics of torsional deflections are shown for ξ varying from 2 to 6. As observed earlier, sharp peaks in $E[N_{+\delta}(\xi,t)]$ values occur at locations at which $y_{\delta}(0,t)$ values crosses the corresponding threshold levels with positive slope. It is also seen that $E[M_{+\delta}(\xi)]$ values are increased due to coupling with blade flapping, a fact also evident from Figure 2b.

5. Concluding Remarks

The previous studies summarized in Reference (2) have shown that high random flapping vibrations and loads must be expected when flying an unloaded rotor at high advance ratio in turbulent air. These flapping random vibrations can be quite effectively alleviated by various feedback systems as was shown in Reference (9). The present study of coupled torsion and flapping random blade vibrations has shown that the problem of random torsional motions and loads at high advance ratio is even more severe than the flapping problem. Even in conditions substantially below the dynamic stability limit, turbulence excited random torsional vibrations are very high. Since the mechanism of these high excitations involves the loss of torsional stiffness through aerodynamic negative spring effects it is difficult to visualize a feedback system which could alleviate the torsional random vibrations and loads. It was found that the aerodynamic coupling between flapping and torsion considerably

aggravates the torsion loads, though only a small effect of this coupling on the flapping loads was established. A more detailed study of the causes of the detrimental coupling may produce some insight into possibilities of devising a type of beneficial coupling which would alleviate the torsional vibrations without substantially increasing the flapping vibrations. The obvious next step is to study the effects of positive and negative δ_3 coupling on the torsional random vibrations.

6. References

1. Gaonkar, G. H., and Hohenemser, K. H., "Flapping Response of Lifting Rotor Blades to Atmospheric Turbulence", Journal of Aircraft, Vol. 6, No. 6, Nov.-Dec. 1969, pp. 496-503.

2. Gaonkar, G. H., and Hohenemser, K. H., "Stochastic Properties of Turbulence Excited Rotor Blade Vibrations", AIAA Journal, Vol. 9, No. 3, March 1971, pp. 419-424.

3. Gaonkar, G. H., and Hohenemser, K. H., "Comparison of Two Stochastic Models for Threshold Crossing Studies of Rotor Blade Flapping Vibrations", AIAA Paper No. 71-389.

4. Sissingh, G. J., "Dynamics of Rotors Operating at High Advance Ratios", J. of A.H.S., Vol. 13, No. 3, July 1968, pp. 56-63.

5. Sissingh, G. J. and Kuczynski, W. A., "Investigation on the Effect of Torsion on the Dynamics of the Flapping Motion", J. of A.H.S., Vol. 15, No. 2, April 1970, pp. 2-9.

6. Lin, Y. K., Probabilistic Theory of Structural Dynamics, McGraw-Hill, 1967, Chapter 9.

7. Roberts, J. B., "Structural Fatigue Under Non-stationary Random Loading", J. of Mechanical Engineering Science, Vol. 8, No. 4, 1966, pp. 392-405.

8. Raiffa, H., and Schlaifer, R. S., Applied Statistical Decision Theory, M.I.T. Press, 1968.

9. Yin, S. K. and Hohenemser, K. H., "The Method of Multiblade Coordinates in the Linear Analysis of Lifting Rotor Dynamic Stability and Gust Response at High Advance Ratio", A.H.S. 27th Annual Forum, May 1971, Paper No. 512.

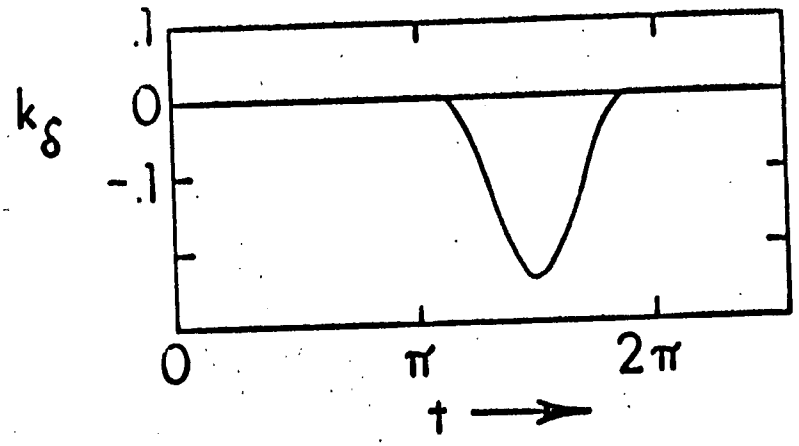

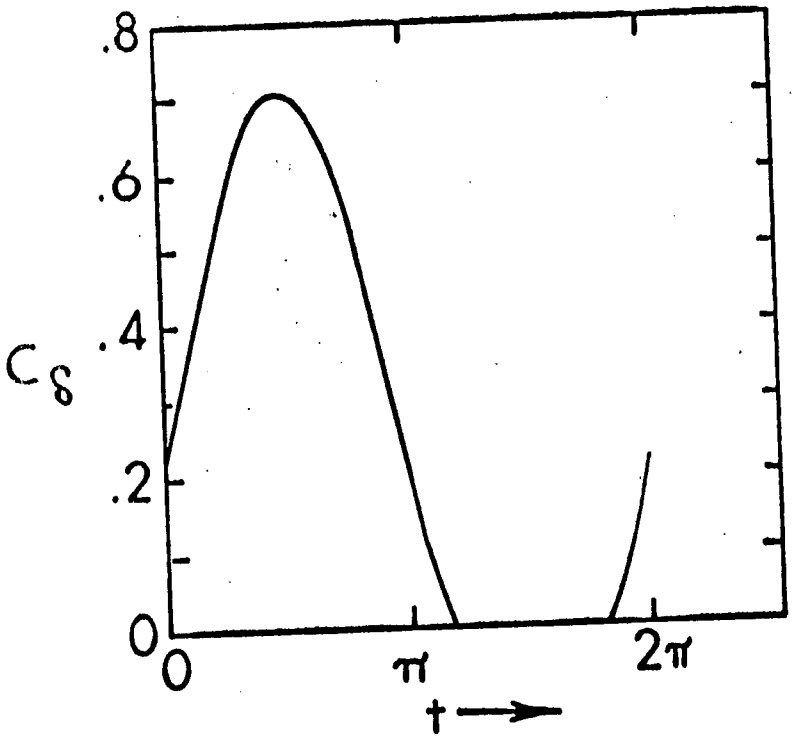

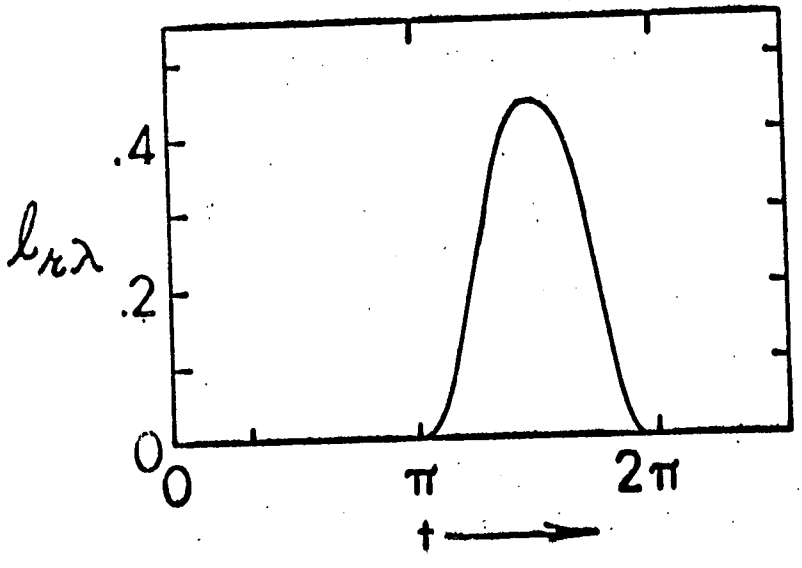

Figure 1a. Periodic System Parameters

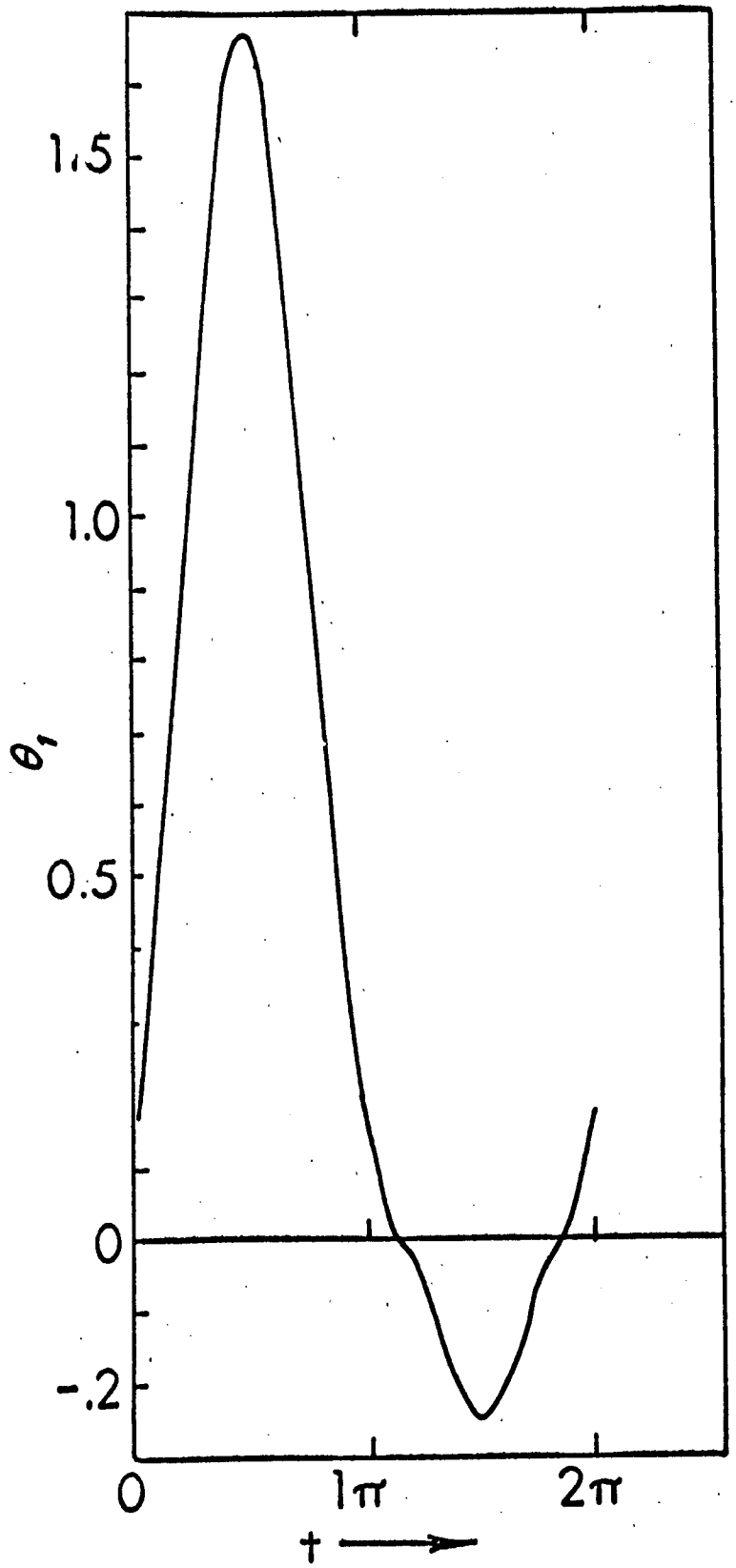

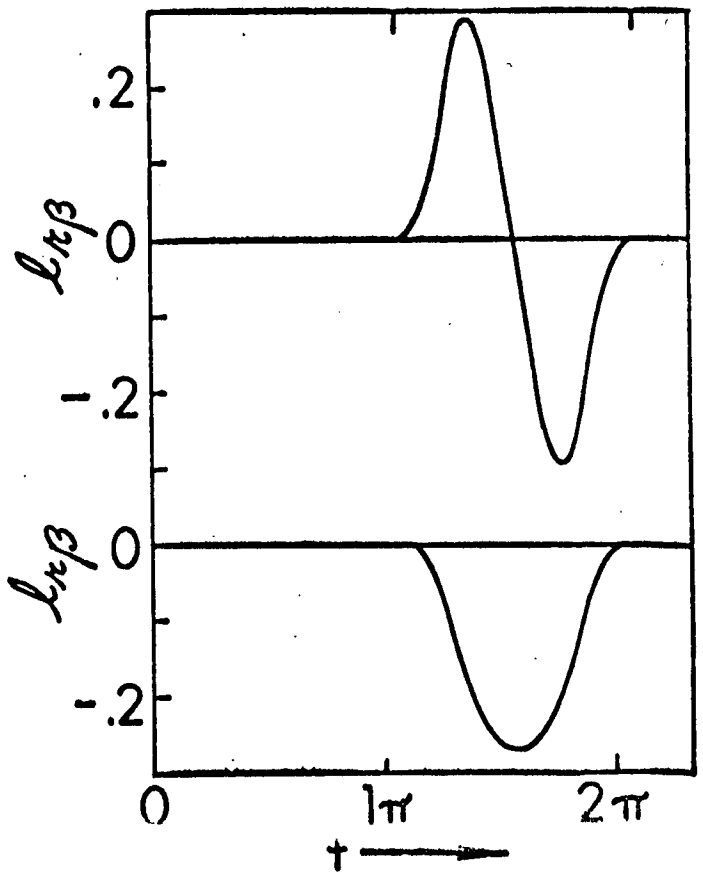

Figure 1b. Periodic System Parameters

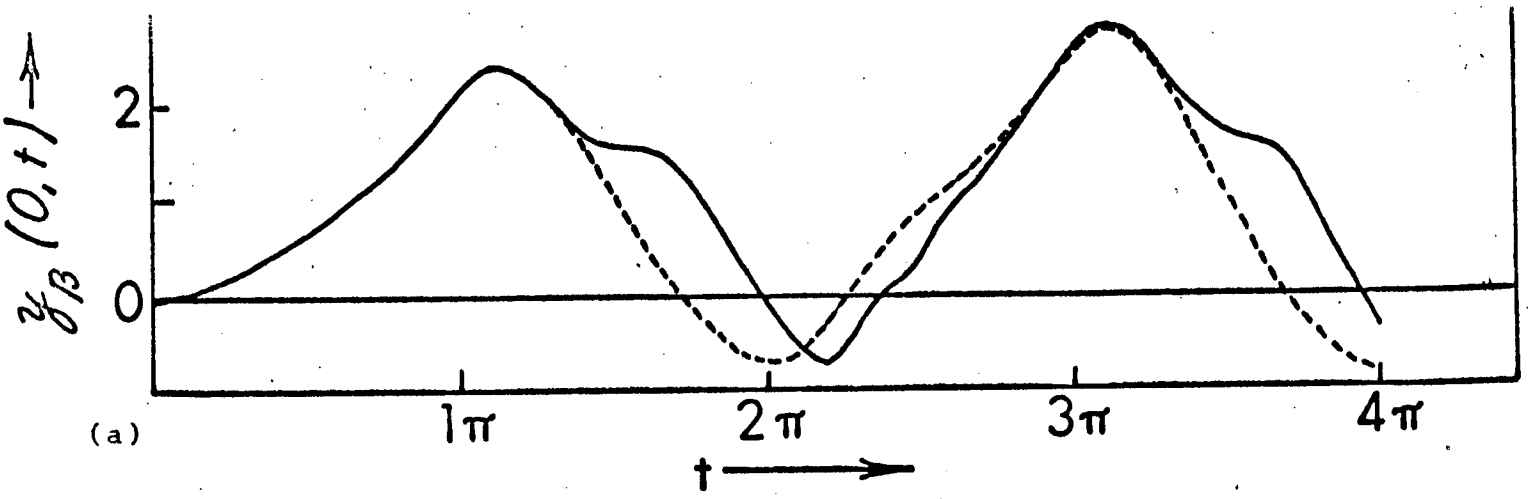

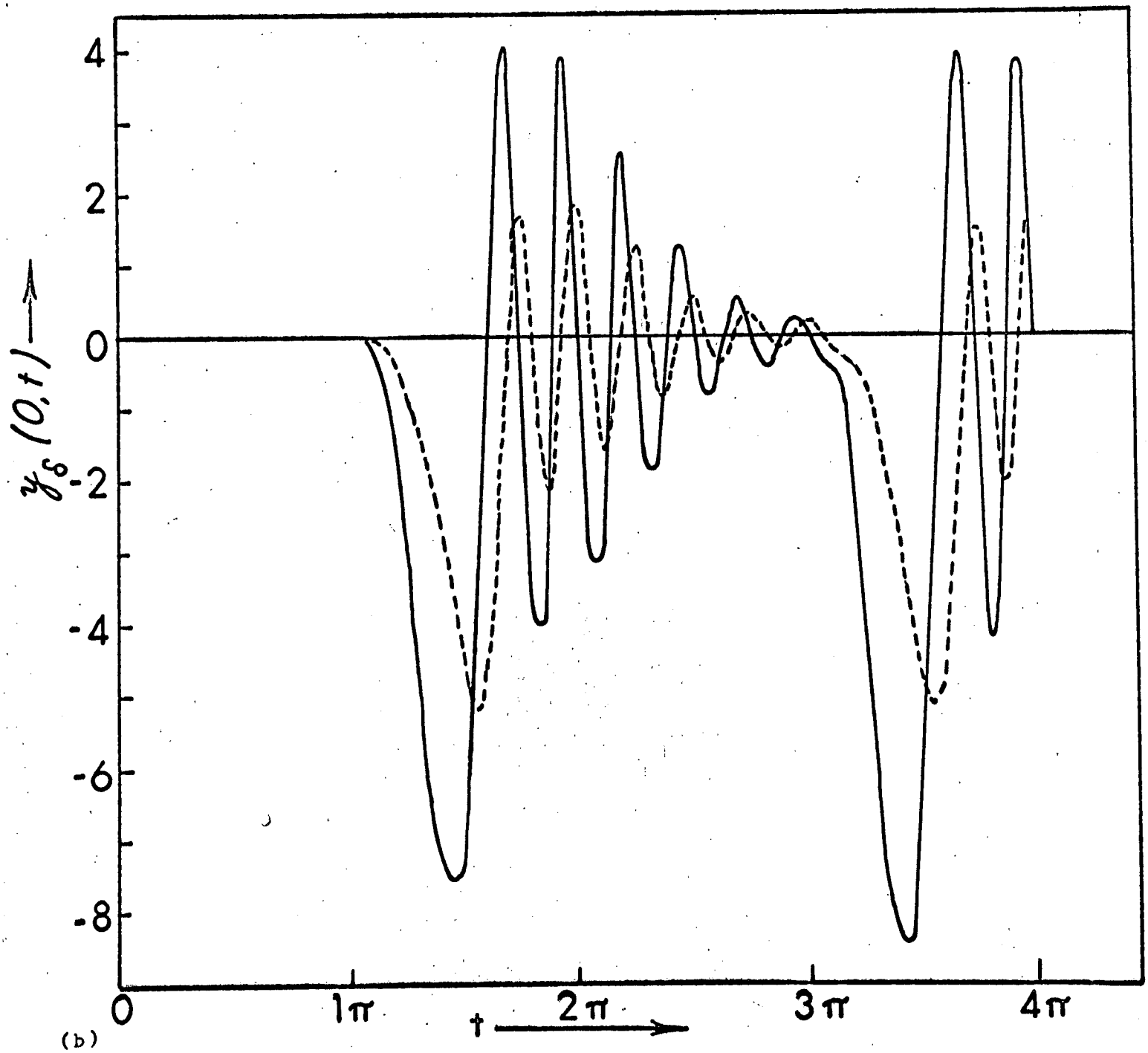

Figure 2. Response to Step Input, Coupled and Uncoupled

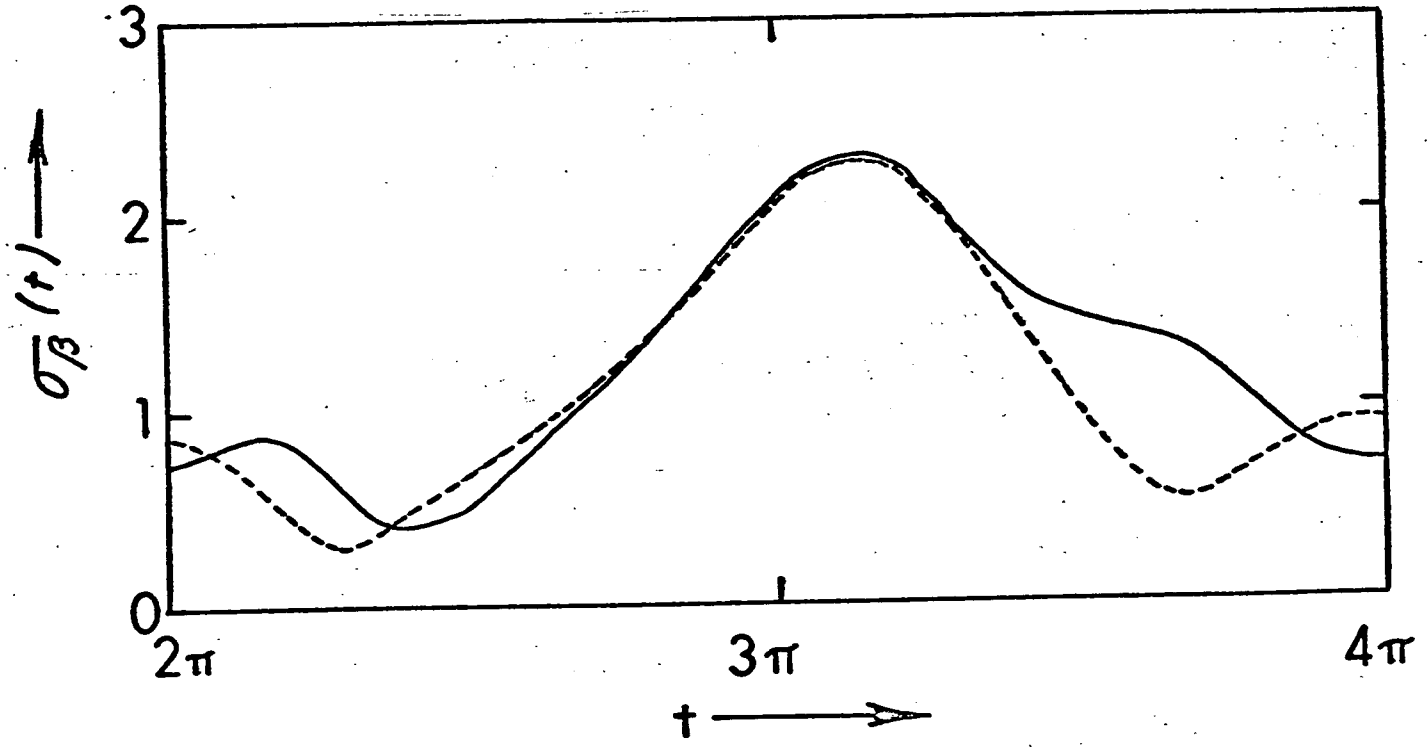

Figure 3. Time Variable Flapping Standard Deviation

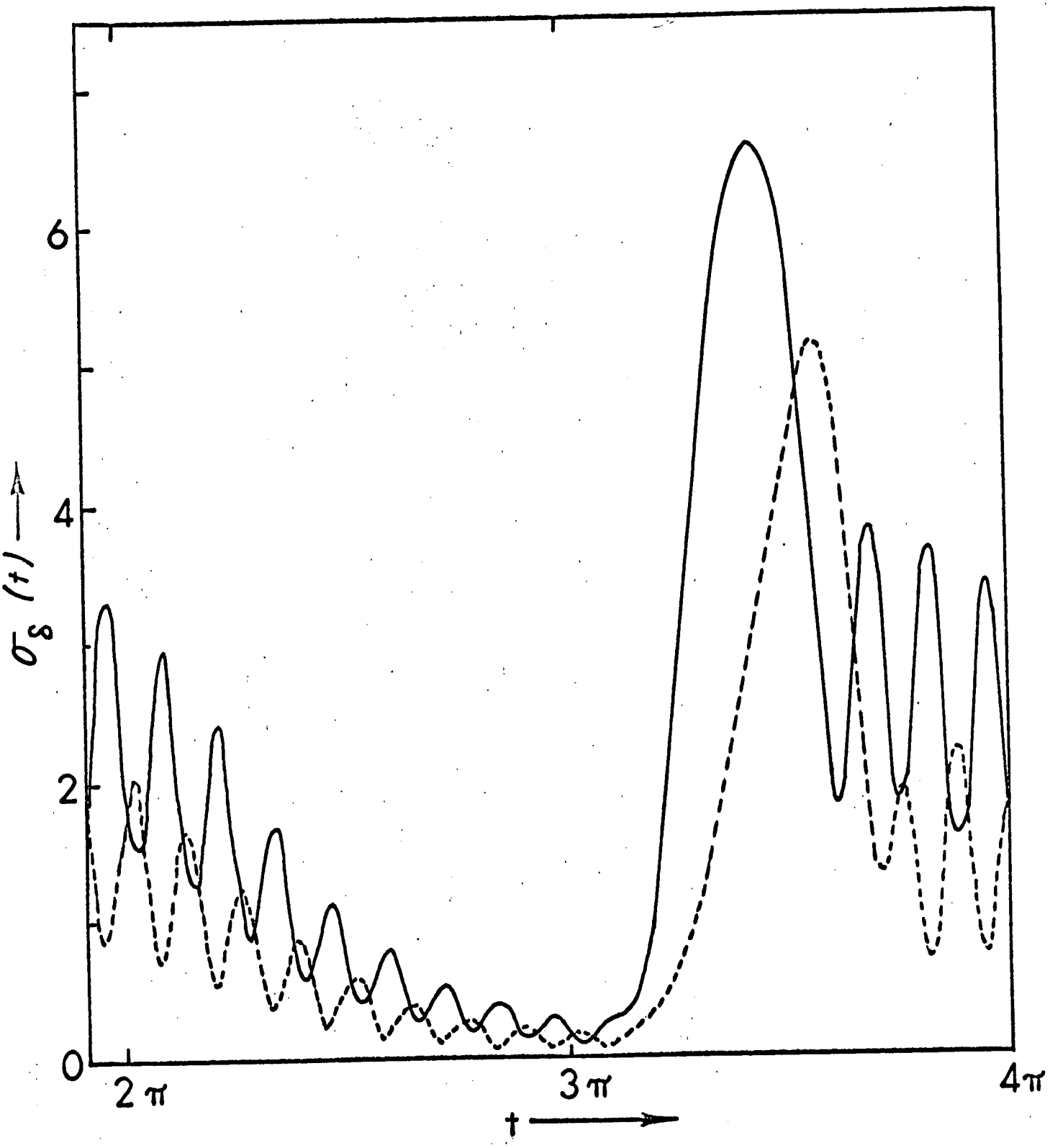

Figure 4. Time Variable Torsion Standard Deviation

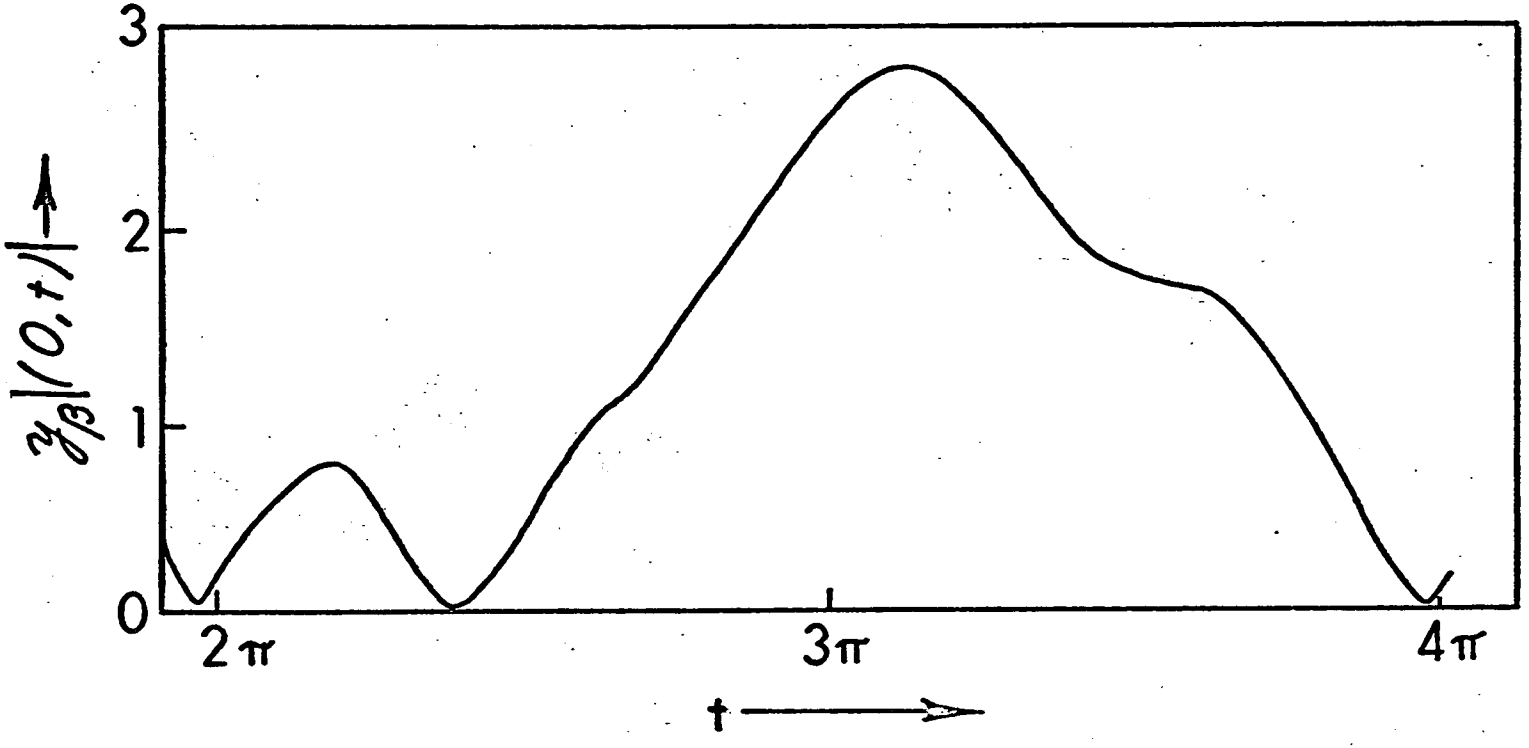

Figure 5a. Time Variable Flapping Standard Deviation for (L/R) = ∞

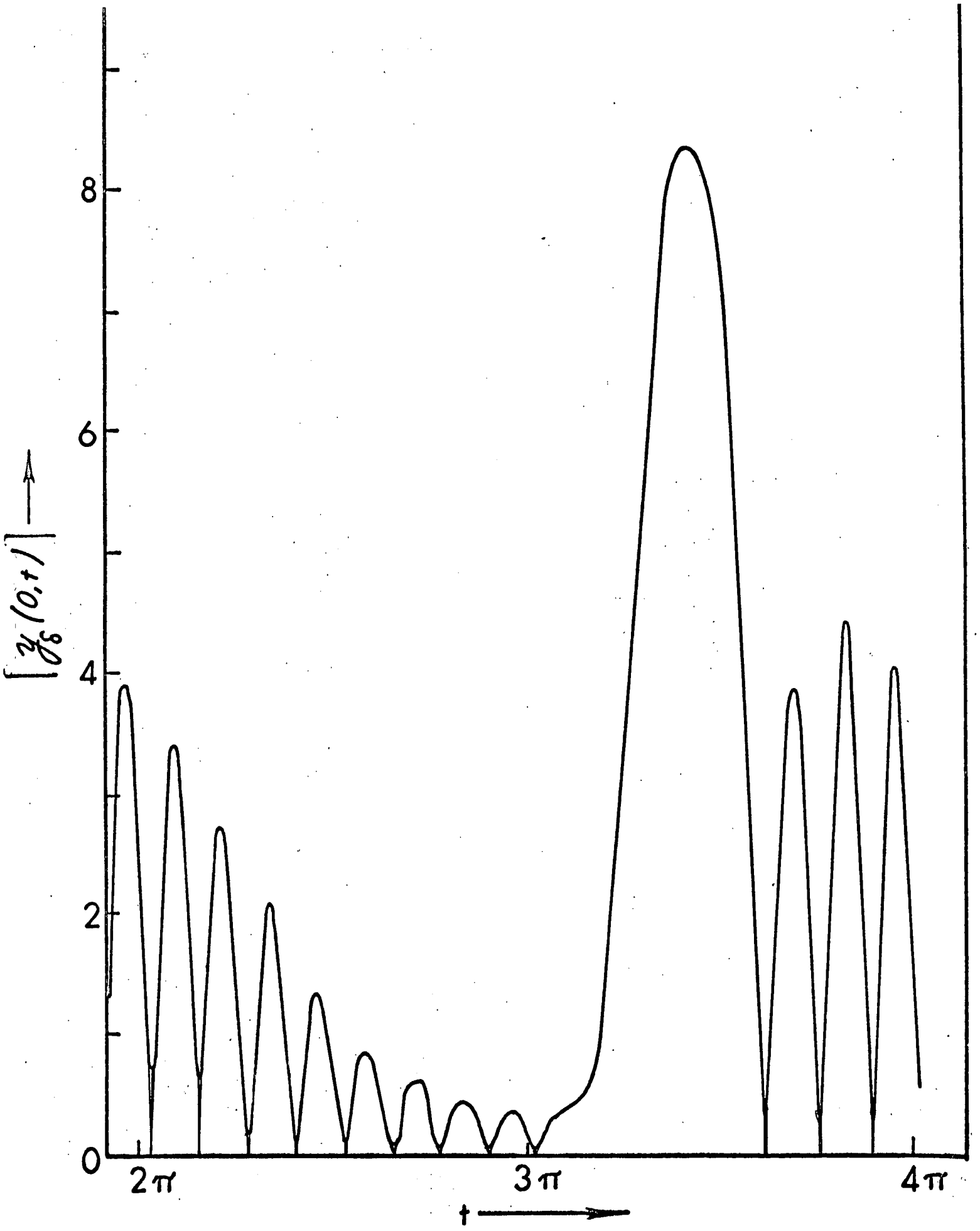

Figure 5b. Time Variable Torsion Standard Deviation for (L/R) = ∞

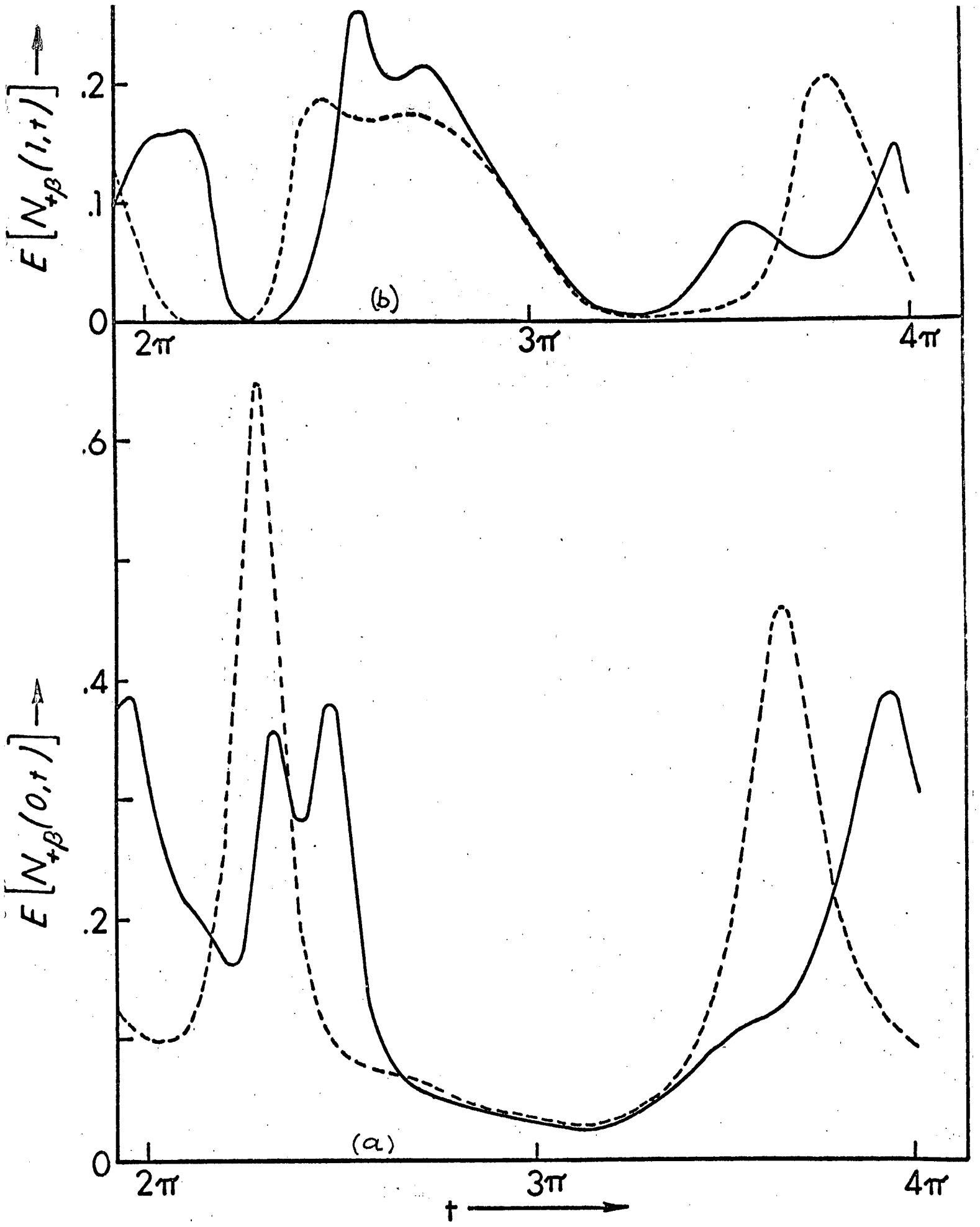

Figure 6. Expected Rate of Flapping Upcrossing of Level Zero (a) and of Level one (b)

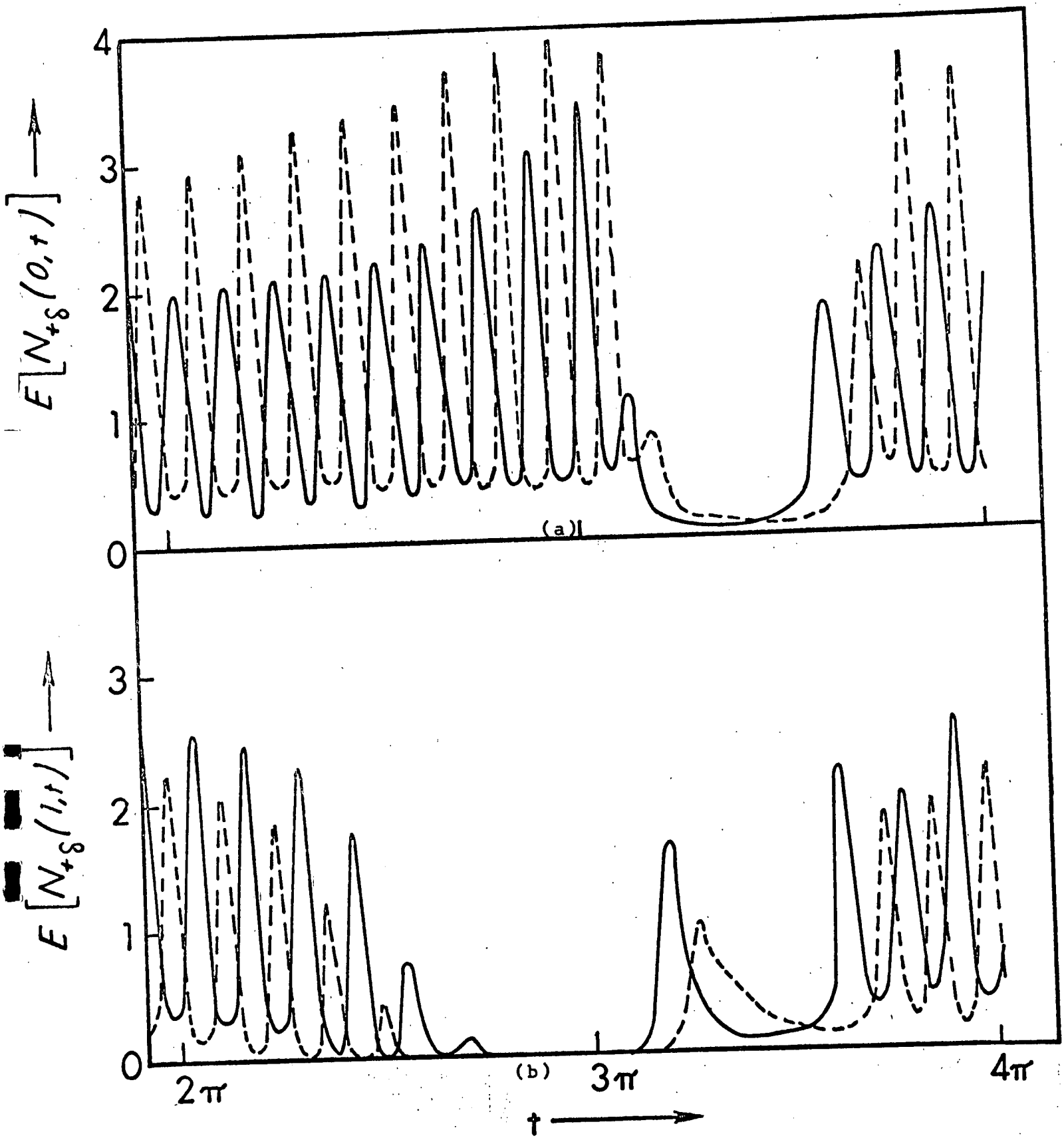

Figure 7. Expected Rate of Torsion Upcrossings of Level Zero (a) and of Level one (b)

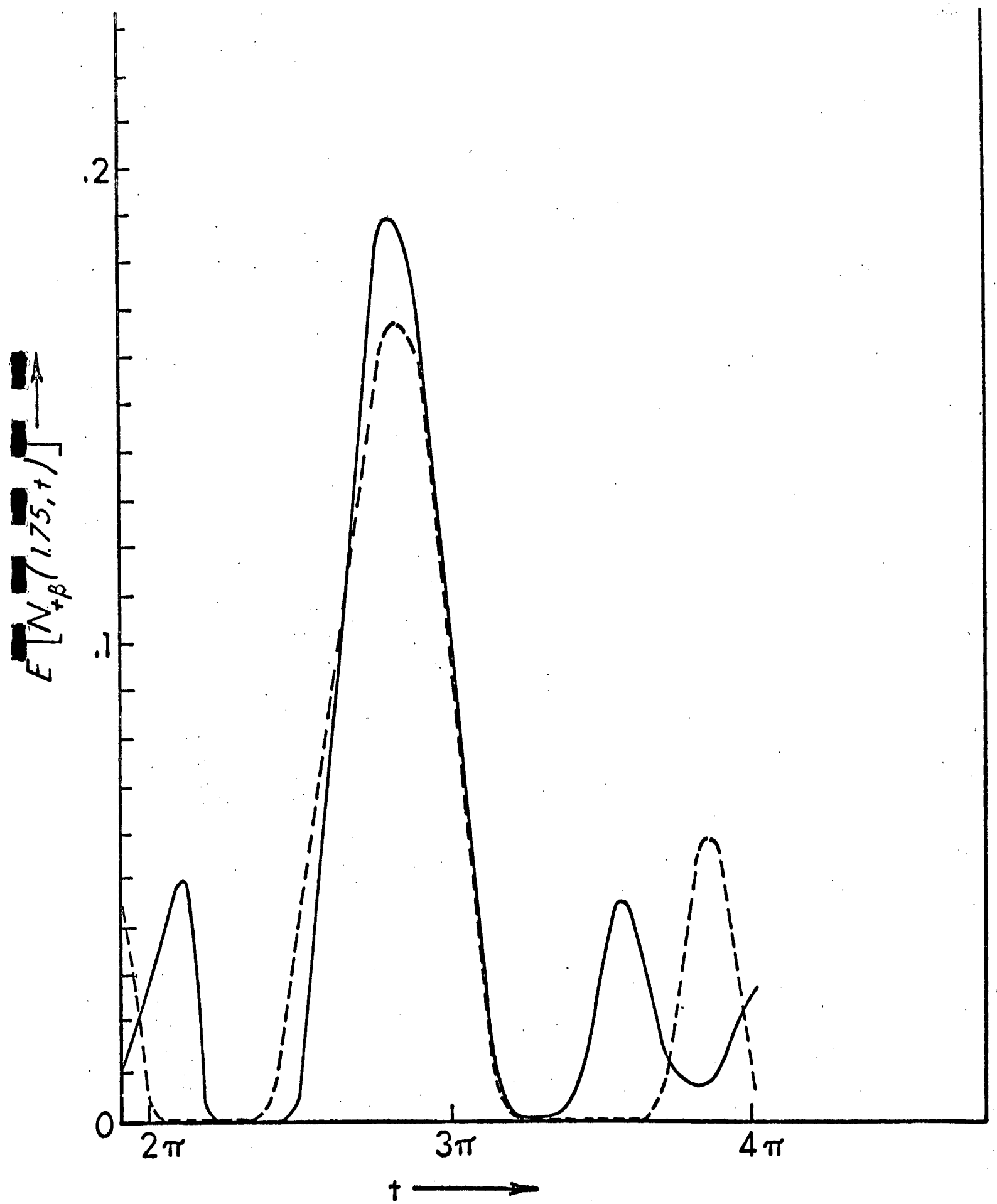

Figure 8a. Expected Rate of Flapping Upcrossings of Level 1.75

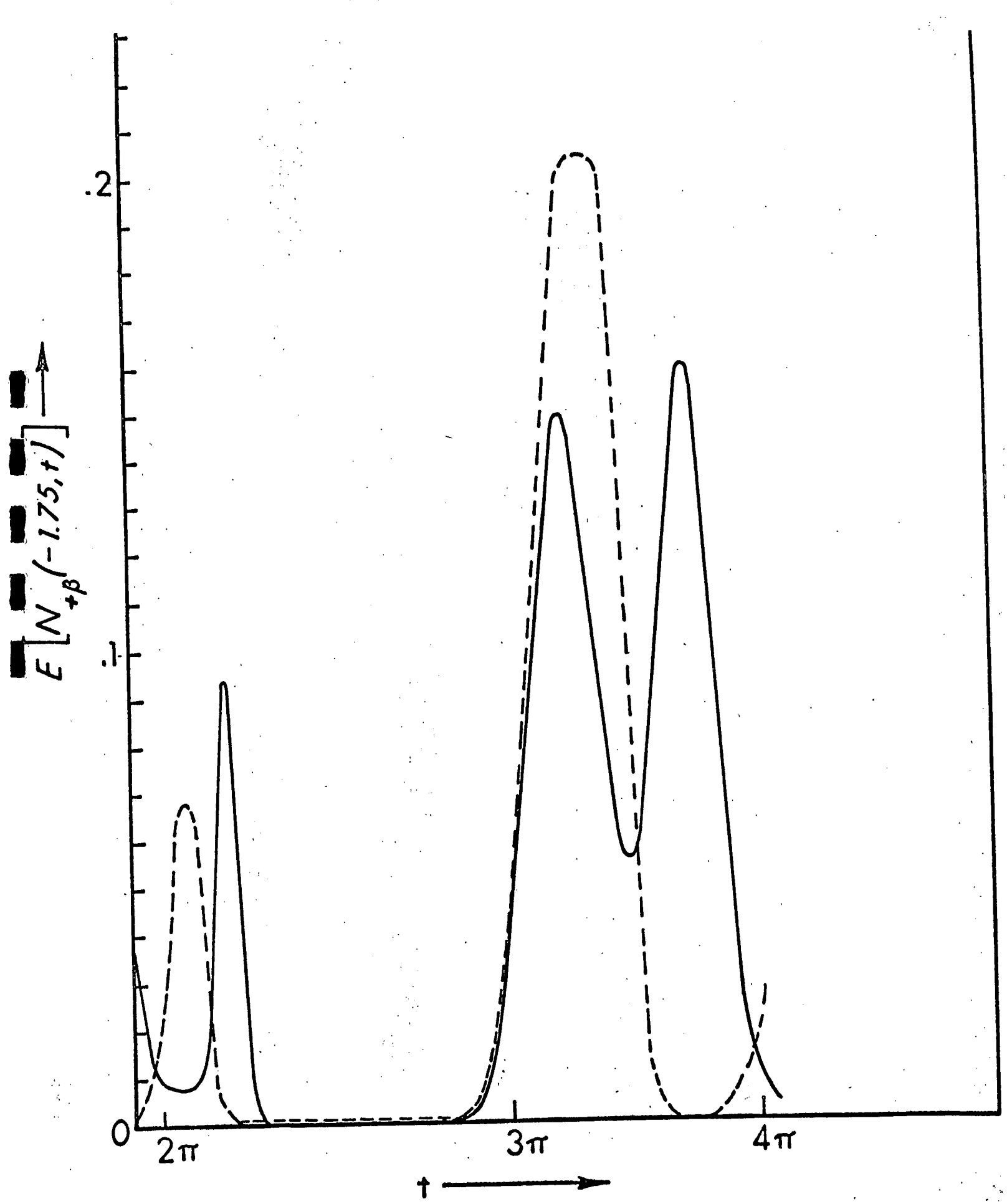

Figure 8b. Expected Rate of Flapping Upcrossings of Level -1.75

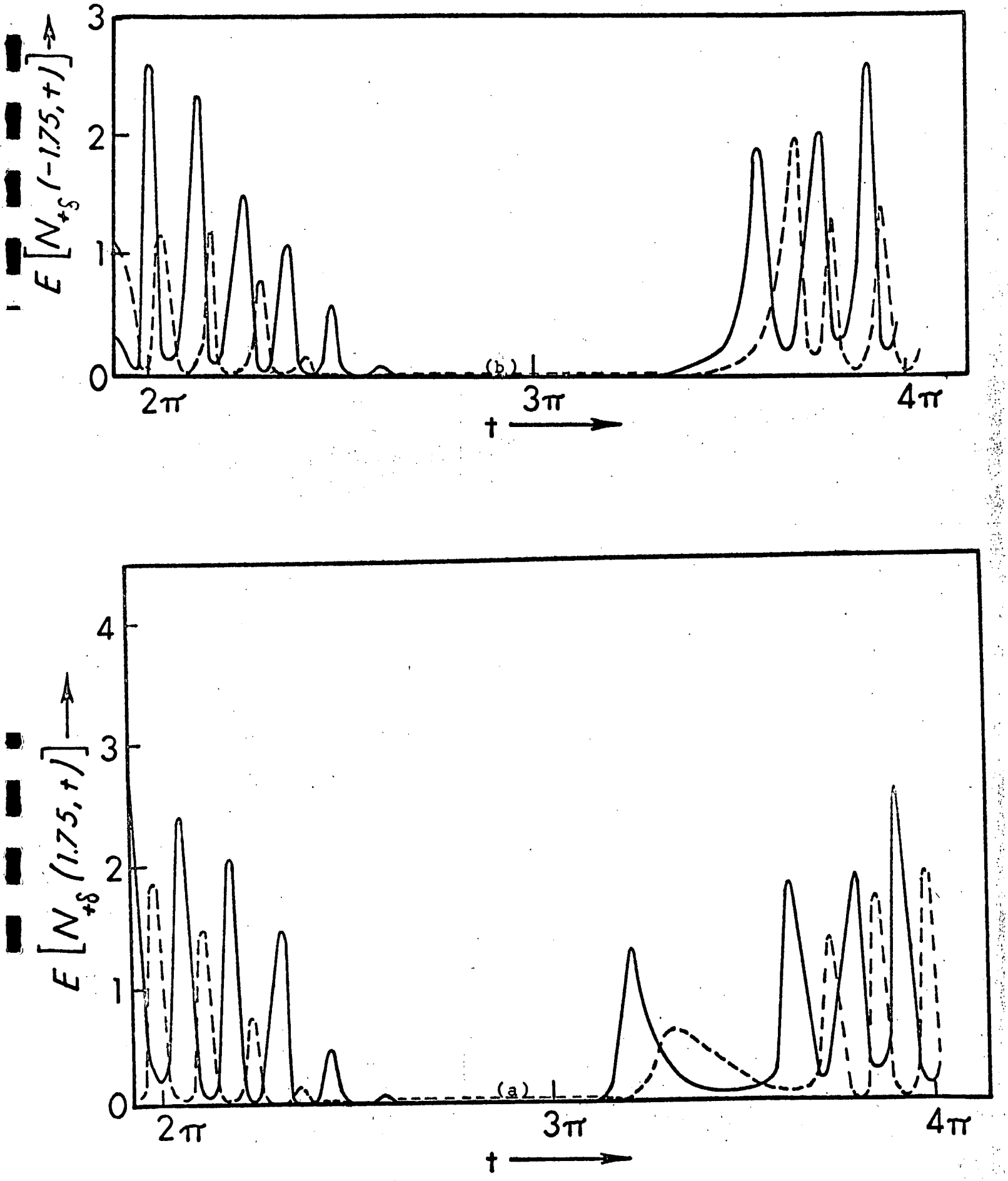

Figure 9. Expected Rate of Torsion Upcrossings of Level 1.75 (a) and of Level -1.75 (b)

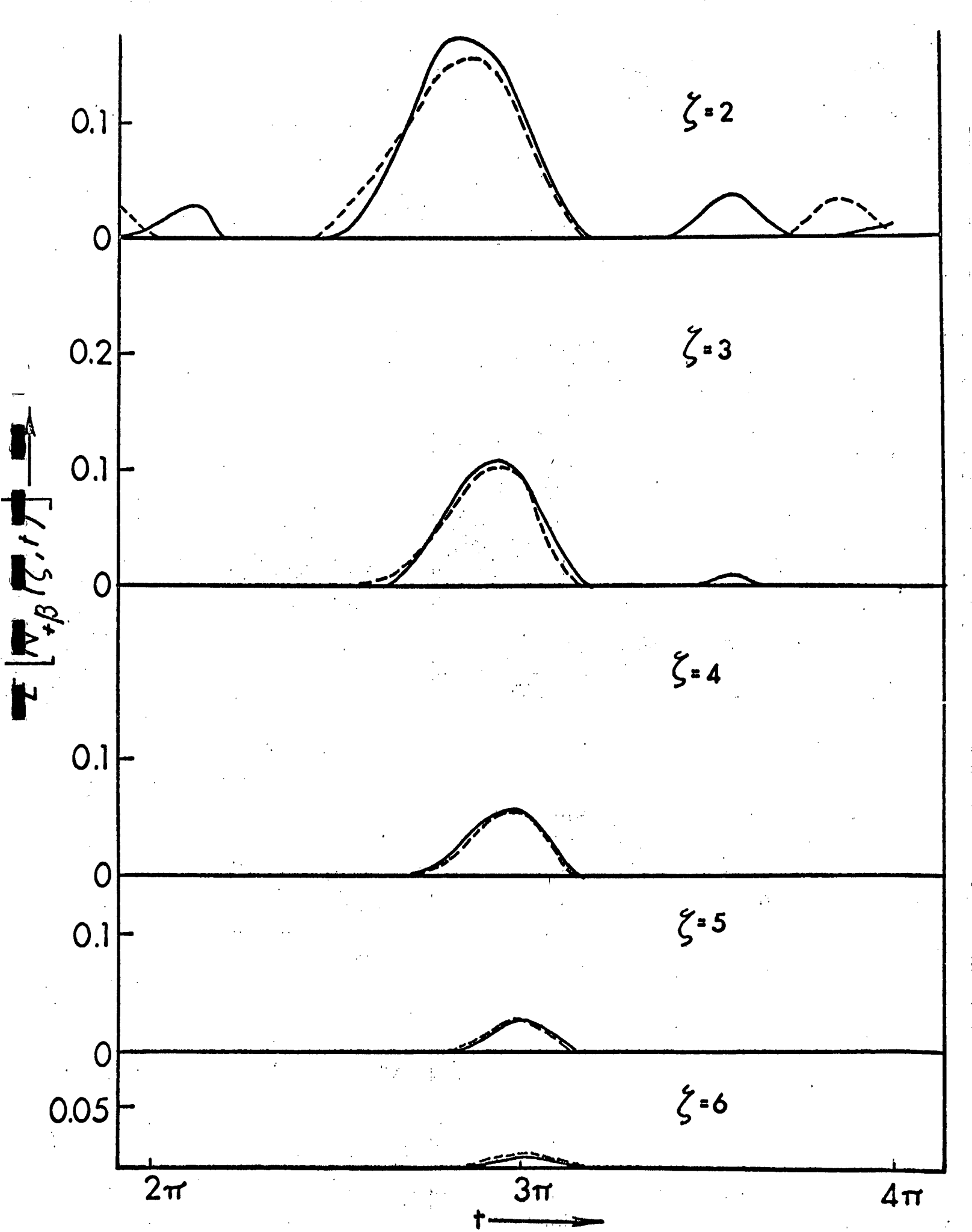

Figure 10. Expected Rate of High Level Flapping Upcrossings

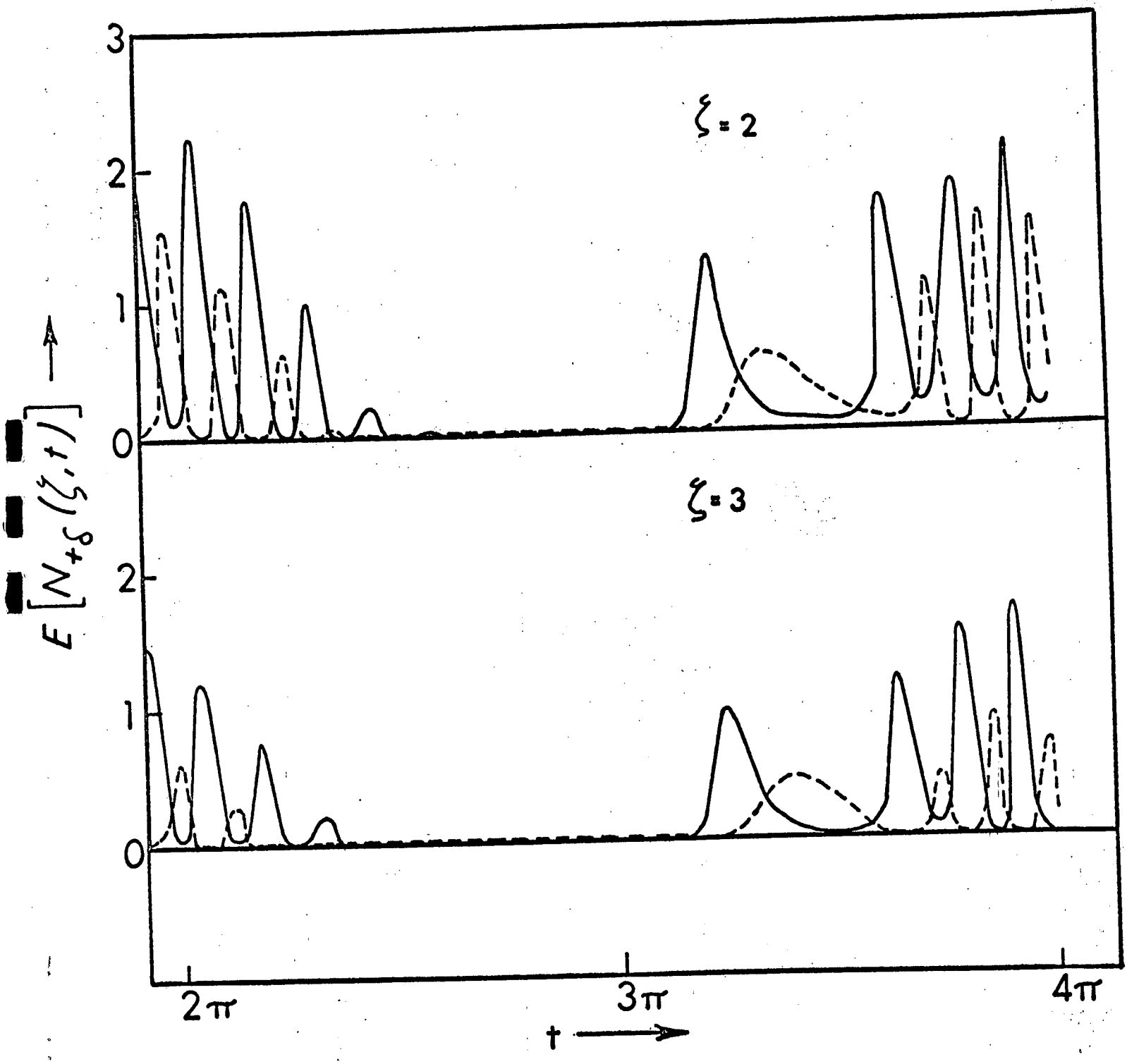

Figure 11. Expected Rate of Torsion Upcrossings of Levels 2 and 3

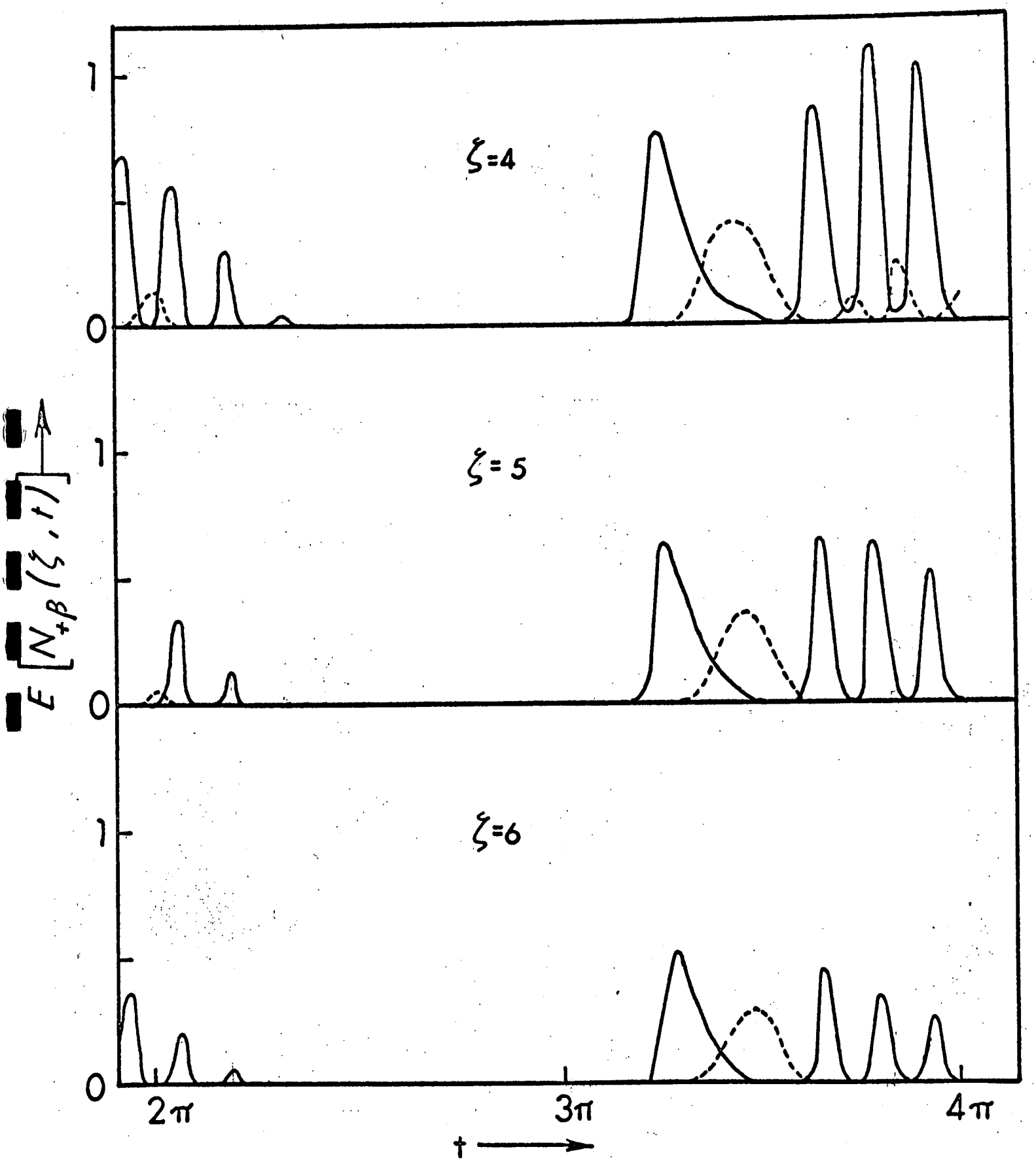

Figure 12. Expected Rate of Torsion Upcrossings of Levels 4, 5, 6.